Response to comments

Referee #2:

General comments: This manuscript presents the development of a compact PERCA–CEAS system for in situ measurements of total peroxy radicals (RO_2), together with its application during a field campaign in Zhuhai. The topic is highly relevant for the atmospheric chemistry community, as direct measurements of peroxy radicals are essential for understanding ozone formation processes. The reported detection limit (~0.2 pptv) and successful field deployment demonstrate promising instrument performance.*
Overall, the manuscript contains valuable results; however, I believe that major revisions are required before publication. My main concerns relate to the description and validation of the measurement technique, particularly the chain length (CL) calibration, as well as some conceptual simplifications and inconsistencies in the instrument description. I also suggest improvements in clarity and language throughout the manuscript.
Response: Thank you for the valuable comments. We have fully considered your concerns, improved the chain length calibration experiment and clarified the instrument description throughout the manuscript. The detailed results are presented in our response letter. **As detailed below, the reviewer's comments are in** *italicized font*, **our response to the comments are shown as** normal font**. New or modified texts are in** blue**.**

Comment [2-1]: ***Definition and terminology of RO_2****. *Lines 15 and 42: It may be more precise to define RO_2* as HO_2+ ΣRO_2, rather than HO_2 + RO_2. It would also be helpful to ensure consistent treatment of RO_2* as a sum of radical species throughout the manuscript.*
Response [2-1]: Thank you for the suggestion. We have redefined RO_2* as "$HO_2 + \sum RO_2$" in lines 15 and 42, and ensured consistent terminology throughout the manuscript.

Comment [2-2]: ***Chain length (CL) calibration and radical interferences.*** *The CL calibration described in Section 2.2 may introduce a systematic overestimation of CL. Photolysis of H_2O produces both OH and H radicals, which may introduce OH into the reactor. If OH reaches the inlet, it can participate in amplification (starting with R4) but is not accounted for in the S_2 signal.*
A possible validation approach would be to add sufficient CO in the HO_2 source to convert OH into HO_2. Extra caution should be taken while adding CO to the source to avoid CL interference coming from the added CO triggering chain reaction in the background mode. It should also be acknowledged that PERCA systems amplify OH and RO radicals, which may become relevant during calibration conditions.
Response [2-2]: Thank you for pointing out this issue. To address the potential

systematic overestimation of CL caused by OH radicals, we redesigned the calibration setup. In this optimized configuration, CO (or N_2 for background mode), originally introduced at the front of the Nafion reactor, is premixed with synthetic air and then introduced immediately downstream of the H_2O photolysis zone, allowing rapid mixing with the photolysis products. This facilitates the prompt conversion of both OH and H radicals into HO_2, while minimizing potential wall losses of radicals before they enter the reactor. During the calibration, the total sampling flow rate and the concentrations of NO and CO within the Nafion reactor remained strictly consistent with our previous experimental conditions.

The revised calibration procedure and signal recording logic are as follows: When the mercury lamp is turned on, CO is introduced upstream in the amplification mode, ensuring that OH is quantitatively converted into HO_2. The total HO_2 concentration is twice that derived from $H+O_2$ pathway alone. The corresponding NO_2 signal is recorded as S_1, which represents the amplified NO_2 produced through the chain reaction initiated by this total HO_2. In the background mode with the lamp still on, N_2 is substituted for CO upstream. In the absence of CO within the reactor, the chain reaction is not triggered and only the HO_2 derived from $H+O_2$ pathway reacts with NO. The corresponding signal in this mode is recorded as S_2. Subsequently, when the mercury lamp is turned off, the NO_2 signals are recorded as S_3 and S_4 under the same amplification and background gas flow conditions, respectively. Consequently, the Chain Length is determined by the formula $CL = (S_1 - S_3) / [2 (S_2 - S_4)]$.

Using this revised procedure, we found that the overestimation of CL associated with OH-derived HO_2 is 47%, and the effective chain length is determined to be 30 ± 2 under our calibration conditions. Accordingly, we have updated the procedures described in Section 2.2 and revised the optimal CL results shown in Section 3.1.

Section 2.2:

"In this work, CL was determined using on-site peroxy radical calibration sources based on water vapor photolysis. A pen-type Hg lamp was used to photolyze H_2O in an N_2 carrier gas (mixture of dry and humidified N_2), producing H atoms and OH radicals (R5). Immediately downstream of the lamp, a mixture of synthetic air and reagent gases (CO/N_2 or CH_4/N_2) was introduced to allow rapid mixing with the photolysis products and reduce radical wall losses. In this configuration, H atoms react with O_2 in the synthetic air to form HO_2 (R6), while the reagent gases control the radical composition. When CO is used as the reagent gas, OH radicals are quantitatively converted to HO_2 (R4), providing a HO_2 calibration source without interference from OH and RO_2 radical."

"The CL was determined using four distinct NO_2 signals detected by the CEAS. For the pure HO_2 source, the Hg lamp was switched on and CO was introduced immediately behind the H_2O photolysis zone, with NO at the inlet of Nafion reactor. Under these conditions, both H atoms and OH from H_2O photolysis were promptly converted to HO_2, then titrated by NO to form NO_2. The resulting NO_2 signal is denoted as S_1 (amplification mode). In the background mode, the lamp remained on while CO was substituted by N_2. The corresponding NO_2 signal, S_2, represents the background mode when HO_2 is only produced by $H+O_2$ pathway. With the lamp off, signal S_3 and

S_4 correspond to the amplification and background signals in the absence of radicals, respectively. Thus, (S_2 – S_4) represents the HO_2 only produced by H+O_2 pathway, whereas (S_1 – S_3) corresponds to the chain-amplified NO_2 signal from HO_2 produced via both the H + O_2 and OH + CO pathways. The CL is then obtained from these four signals using Eq. (2).

$$CL = \frac{\Delta NO_2}{[HO_2]} = \frac{S_1 - S_3}{2(S_2 - S_4)} \qquad (Eq.2)$$

”

Section 3.1:

“

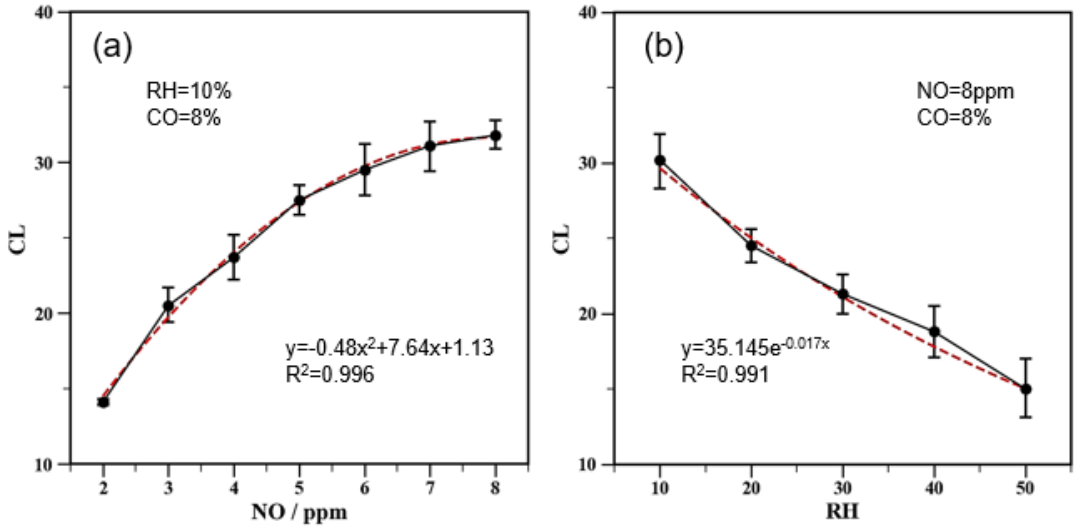

Figure 2. (a) Relationship between the CL and NO concentration under conditions of 10% RH and 8% CO concentration. (b) Variation of CL with RH at a fixed NO concentration of 8 ppm and CO concentration of 8%. (Error bars represent the standard deviation of five independent measurements.)

”

“The optimal CL for the PERCA-CEAS measurement system was determined to be 30±2 under the conditions of RH = 10%, NO = 8 ppm, and CO = 8% based on the pure HO_2 calibration.”

Comment [2-3]: ***Representativeness of CL for RO_2 species.*** *CL for RO_2 is generally lower than for HO_2, and this difference depends strongly on system-specific factors such as wall losses and reactor design. Therefore, adopting uncertainties from other instruments* (Kartal et al., 2010) *may not be appropriate without justification. The authors should consider calibration with at least one RO_2 species or clearly state this as a limitation.*

Response [2-3]: Thank you for the comment. We performed a dedicated calibration using methyl peroxy radicals (CH_3O_2) in addition to the standard HO_2 source. Specifically, a mixed HO_2–CH_3O_2 calibration source was generated by replacing CO with CH_4 (150 ppm in N_2) immediately downstream of the H_2O photolysis zone. In this configuration, OH radicals react with CH_4 to form CH_3O_2 via $OH + CH_4 + O_2 + M \rightarrow CH_3O_2 + H_2O + M$, while H atoms are efficiently converted to HO_2. The setup is

expected to yield a mixture of 50% HO_2 and 50% CH_3O_2. Our results show that the CL derived from this mixed source differs from that obtained using the pure HO_2 source by 20%, with a measured CL of 24.

These details have been added in Sections 2.2 and 3.1, and the resulting uncertainty has been incorporated into the overall uncertainty budget (Section 3.2).

Sections 2.2:

"…RO_2 radical. When CH_4 (150 ppm in N_2) is used instead of CO, OH reacts with CH_4 to form CH_3O_2 (R7), yielding a mixed peroxy radical source containing approximately 50 % HO_2 and 50 % CH_3O_2 under typical calibration conditions."

"…using Eq. (2). The mixed HO_2–CH_3O_2 standard was generated by introducing CH_4 only during the S_1 (amplification) measurement and was used to verify the instrument response to organic peroxy radicals relative to HO_2 under otherwise identical conditions."

Sections 3.1:

"…HO_2 calibration. Calibration using a mixed radical source consisting of 50% HO_2 and 50% CH_3O_2 yielded a CL of 24±1 under the same conditions."

Sections 3.2:

"(3) Uncertainty in radical partitioning. This arises from variability in the relative contributions of HO_2 and CH_3O_2 to total peroxy radicals. Based on the reported HO_2/RO_2 (0.8–1.2) and CH_3O_2/RO_2 (0.85–0.95) ratios from Stone et al., (2010), the mole fraction of CH_3O_2 in total peroxy radicals (f) is estimated to be 0.41–0.54. Under these conditions, the use of an HO_2-based calibration would introduce a systematic bias of 16–22% in the derived RO_2* concentration."

Comment [2-4]: ***Instrument description***. *As this is the first publication of the PWRCA system used, additional details such as flow rate, residence time, reactor pressure, detector flow conditions, etc should be included for reproducibility.*

Response [2-4]: Thanks for the suggestions. We have clarified additional details of technical specifications in Section 2.1, such as reagent gas purities, flow rates, mixing ratios, reactor dimensions, and residence times. The revised text is as follows:

"The NO and CO gases were injected into the system accompanied by N_2 as a balancing gas. To ensure gas purity, the NO (100 ppmv in N_2) was passed through a ferrous sulfate heptahydrate ($FeSO_4 \cdot 7H_2O$) filter to remove trace NO_2 impurities. The flow rate of this NO mixture was regulated at 120 mL/min, achieving a final concentration of 8 ppmv in the reactor. Similarly, high-purity CO gas (99.99%) was passed through an activated carbon column to eliminate residual carbonyl compounds before entering the reactor at 120 mL/min, corresponding to a constant concentration of 8% (v/v) during amplification mode. The total system flow was maintained at 1500 mL/min using mass flow controllers, corresponding to a residence time of approximately 3 s in the reaction zone."

Comment [2-5]: ***Valve configuration.*** *There is inconsistency between the text and schematic regarding valve configuration.*

- *Line 156 refers to one three-way solenoid valve,*

- *Figure 1 shows four two-way valves*

- *Line 160 also mentions four solenoid valves.*

This should be clarified.

Response [2-5]: Thanks for the careful check of the valve configuration. We apologize for the inconsistency in the description of the valve configuration. The system actually uses four two-way solenoid valves instead of three-way valves. The text has now been revised to ensure consistency with Figure 1. We have updated the description in Section 2.1 to explicitly state this configuration.

"To enable automated switching between amplification and background modes in the single-channel configuration, an automatic valve-switching module driven by a programmable timer was developed. The flow paths of CO and N_2 were controlled using four two-way solenoid valves, with two valves assigned to each gas line. During the amplification mode, the timer directs CO to the front inlet to initiate the chain reaction with NO, while N_2 is routed to the rear inlet. Conversely, in the background mode, the valve states are toggled so that N_2 is introduced at the front and CO is directed to the rear. By synchronizing the switching of these four valves, the system achieves stable and automated mode transitions for real-time detection of peroxy radicals."

"

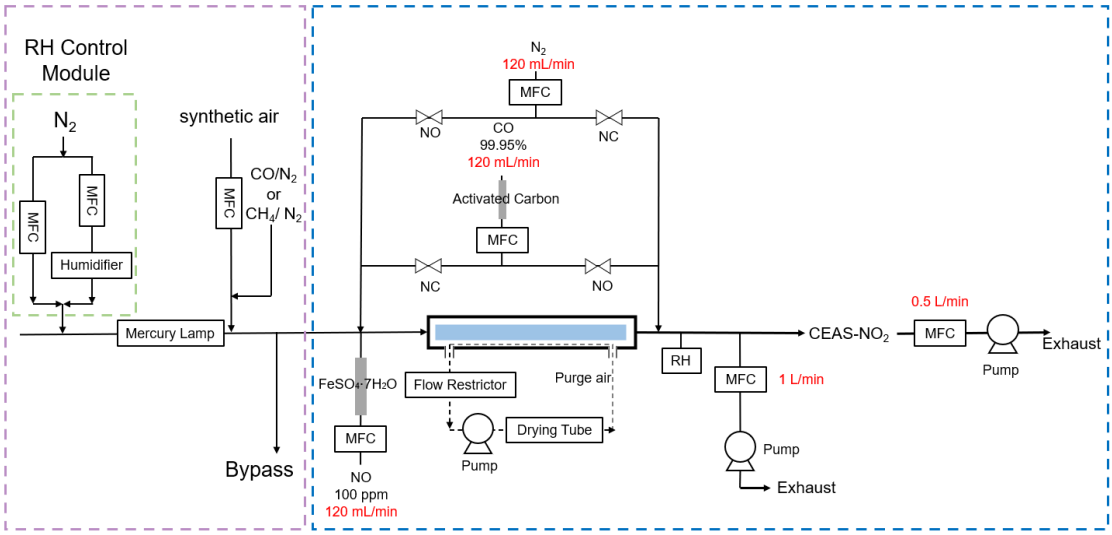

Figure 1. Schematic diagram of the PERCA-CEAS system. The purple dash line portion represents the standard source module, which consists of the standard gas generation unit and the relative humidity (RH) control unit (outlined in green) and is used for calibrating the system chain length. The blue dash line portion represents the measurement module, comprising the chemical amplification unit and the NO_2 detection unit, which together enable the quantification of atmospheric peroxy radicals.

"

Comment [2-6]: *HO_2 source in the schematic diagram. The schematic suggests N_2 is humidified prior to photolysis, but HO_2 formation requires O_2. The authors should clarify how O_2 or synthetic air is introduced and whether it is always present. The*

publication will benefit from including additional details about the source (e.g. Flow rates)

Response [2-6]: Thanks for the suggestions. To ensure rapid conversion of both H atoms and OH radicals to HO_2, a mixture of synthetic air and reagent gases (CO/N_2 or CH_4/N_2) is injected immediately downstream of the photolysis zone within the calibration module. This ensures that O_2 is always present to promote radical conversion and minimize potential wall losses. In addition, the relative humidity (RH) of the radical standard source was maintained at approximately 10% by adjusting the mixing ratio of dry and humidified N_2 streams, while providing a stable radical output of ~1–3 ppbv.

We have updated Section 2.2 and Figure 1 in the revised manuscript to reflect these modifications.

"…water vapor photolysis. A pen-type Hg lamp was used to photolyze H_2O in an N_2 carrier gas (mixture of dry and humidified N_2), producing H atoms and OH radicals (R5). Immediately downstream of the lamp, a mixture of synthetic air and reagent gases (CO/N_2 or CH_4/N_2) was introduced to reduce radical wall losses and allow rapid mixing with the photolysis products."

"…calibration conditions. In all cases, the relative humidity in the calibration flow was adjusted to ~10 %, yielding a stable peroxy radical concentration of ~1–3 ppbv."

"

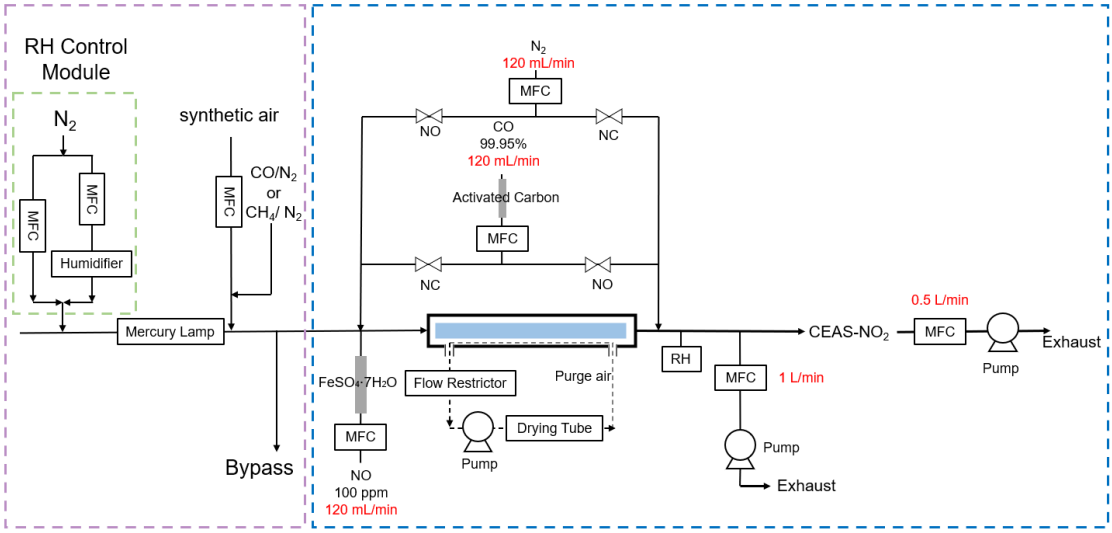

Figure 1. Schematic diagram of the PERCA-CEAS system. The purple dash line portion represents the standard source module, which consists of the standard gas generation unit and the relative humidity (RH) control unit (outlined in green) and is used for calibrating the system chain length. The blue dash line portion represents the measurement module, comprising the chemical amplification unit and the NO_2 detection unit, which together enable the quantification of atmospheric peroxy radicals.

"

Comment [2-7]: ***PERCA interferences.*** *A discussion of PAN thermal decomposition and related interferences would improve the scientific completeness.*

Response [2-7]: Thanks for the suggestion. The potential interference from PAN thermal decomposition was evaluated using a F0AM model (Framework for 0-D

Modeling) under the experimental conditions (26.5 °C and 3 s residence time). The simulations indicate that the chemical amplification process is highly time-limited, reaching near completion within approximately 0.15 s. Within this short reaction window, only a fraction of PAN-derived radicals can effectively participate in the chain propagation before being removed by wall losses or exiting the reaction zone. Importantly, any NO_2 produced from slower PAN thermal decomposition outside the effective reaction window is also present in both amplification and background modes and is therefore removed through the differential measurement approach. Under a representative PAN level of 1.0 ppbv, the interference generated within the effective reaction window corresponds to an equivalent RO_2* signal of ~1.95 pptv. This accounts for approximately 1.3–9.8% of the typical RO_2* concentrations (20–150 pptv) observed during the campaign and has been incorporated into the overall measurement uncertainty.

We have added a detailed discussion regarding the potential interference from PAN thermal decomposition in Section 3.2 of the revised manuscript.

"(4) PAN interference. The thermal decomposition of PAN represents a potential source of interference, as it releases NO_2 and peroxy radicals that can trigger additional chemical amplification within the reactor (Liu and Zhang, 2014; Wood and Charest, 2014). Kinetic simulations using the F0AM model (Framework for 0-D Modeling; Wolfe et al., 2016) indicate that 1.0 ppbv PAN results in an equivalent RO_2* signal of 1.95 pptv under our experimental conditions (26.5 °C and a amplification reaction time of 0.15 s). This accounts for 1.3–9.8% of the typical RO_2* levels (20–150 pptv) observed during the campaign."

Comment [2-8]: ***Interpretation of chain length comparisons.*** *CL comparisons should consider reactor material, reactor design, working pressure, humidity, and wall losses. Instruments such as* Horstjann et al., (2014) *include pre-reactor chambers that increase wall losses. The comment about influence of detection technique on CL should be reconsidered.*

Response [2-8]: Thanks for the suggestion. To address this, we have revised Section 3.1 and added Table 1 to provide a detailed summary of calibration conditions and technical specifications for previous PERCA systems.

"As summarized in Table 1, the obtained CL is lower than values reported in most previous PERCA studies, which were typically above 50 and occasionally exceeded 200 (George et al., 2020; Wood and Charest, 2014). The differences in CL are primarily attributed to wall loss of HO_2 radicals due to reactor material, reactor design and working pressure. Although the obtained CL is relatively low compared with these PERCA instruments, our results demonstrate that the developed PERCA-CEAS system provides stable and reliable sensitivity for atmospheric RO_2* measurements.

Table 1. Summary of performance for reported PERCA measurement systems

Measurement System	Channel Configuration	Calibration Source	CL	LOD	Uncertainty	Pressure (mbar)	Reference

PERCA-luminox	Single	CH_3O_2	200-260	2 pptv	40%	400 ~ 1000	(Green et al., 2003)
PERCA-luminol	Dual	HO_2 50%HO_2+50%CH_3O_2	45±7	3±2 pptv (3σ)	/	200	(Kartal et al., 2010)
PERCA-luminol	Dual	HO_2 50%HO_2+50%CH_3O_2	88±17 64±18	3 pptv (1σ)	/	300	(Horstjann et al., 2014)
PERCA-CRDS	Dual	HO_2	150±50	10 pptv (3σ)	/	1000	(Liu et al., 2009)
PERCA-CRDS	Dual	HO_2 CH_3O_2	200 180	4 pptv (3σ)	/	1000	(Liu and Zhang, 2014)
PERCA-CRDS	Dual	HO_2 50%HO_2+50%CH_3O_2	62 ± 9	< 2 pptv	15%	200 ~ 350	(George et al., 2020)
PERCA-CRDS	Dual	HO_2 RO_2*	55	0.9 pptv (3σ)	/	1000	(Duncianu et al., 2020)
PERCA-CAPS	Dual	$CH_3C(O)O_2$ CH_3O_2	168±20	0.6 pptv (1σ, 60s)	25%	1000	(Wood and Charest, 2014)
ECHAMP-CAPS	Dual	$CH_3C(O)O_2$ CH_3O_2	17	2.5 pptv (1σ, 90s)	27%	1000	(Wood et al., 2017)
PERCA-IBBCEAS	Dual	HO_2	91±11	0.9 pptv (1σ)	16-20%	1000	(Chen et al., 2016)
PERCA-CEAS	Single	HO_2 50%HO_2+50%CH_3O_2	30±2 24±1	0.38 pptv (1σ)	18.4-25.7%	1000	This work

”

Comment [2-9]: ***Simplifications in ozone production analysis.*** *The assumption k_eff = k(HO_2+NO) and simplified D(O_3) estimates should be discussed as sources of uncertainty.*

Response [2-9]: Thanks for the suggestion. Considering the uncertainties associated with RO_2* measurements (18.4-25.7%), the k_{eff} approximation (~10%) and the upper limit of D(O_3) level (5%), the overall uncertainty in $P(O_3)_{net}$ is estimated to be 21.5-28.0% according to error propagation calculation. These uncertainty analyses have been added to the revised text in Section 3.4.

“Considering uncertainties associated with RO_2* measurements (18.4-25.7%), the approximation of k_{eff} (~10%), and the upper limit of D(O_3) level (5%), the overall uncertainty in $P(O_3)_{net}$ was estimated to be 21.5-28.0%.”

Comment [2-10]: ***Interpretation of VOC influence.*** *The attribution to VOC reactivity in Line 326 requires supporting evidence or should be presented more cautiously.*
Response [2-10]: Thanks for the suggestion. Although in-situ VOC measurements were not conducted, regional studies suggest relatively high VOC reactivity in the study area. Studies at nearby coastal sites (e.g., Da Wan Shan Island) have reported high oxidative capacity in air masses over the Pearl River Estuary, associated with strong VOC consumption and enhanced radical cycling (Sun et al., 2024). In addition, the subtropical climate and dense vegetation in the Pearl River Delta contribute substantial biogenic emissions (e.g., isoprene), which may enhance the regional radical budget (Situ et al., 2013; Wang et al., 2023c). At our site, these elevated VOC levels are likely to sustain RO_2 formation and reduce sensitivity to NO titration, thereby shifting the RO_2*- NO transition toward higher NO levels. We have strengthened the discussion by adding supporting literature on VOC reactivity in Section 3.3 of the revised manuscript.

"This behavior is consistent with the elevated VOC reactivity inferred for studies conducted near our observation site. Studies at nearby coastal sites (e.g., Da Wan Shan Island) have reported high oxidative capacity associated with strong VOC consumption and enhanced radical cycling (Sun et al., 2024), while the dense vegetation in the Pearl River Delta contributes substantial biogenic VOC emissions (e.g., isoprene) (Situ et al., 2013; Wang et al., 2023c). Collectively, these factors contribute to sustaining propagation cycles of RO_2 radical and shift the turning point of the NO dependence of RO_2* concentration higher at our site."

Comment [2-11]: ***Interpretation nighttime RO_2*.*** *If the nighttime RO_2* is attributed to NO_3 driven chemistry, more detailed scientific explanation is necessary since NO_3 measurement are not given.*
Response [2-11]: Thanks for the suggestion. To provide further clarification, the nitrate radical production rate, $P(NO_3)$, was calculated as follows:

$$P(NO_3) = k[NO_2][O_3]$$

where k_{NO2+O3} represents the temperature-dependent rate constant for the reaction between NO_2 and O_3 (Atkinson et al., 2004). During the campaign, the average nighttime (18:00–06:00) $P(NO_3)$ was approximately 1.4 ppbv·h^{-1}, higher than the reported warm-season mean of 1.07 ± 0.38 ppbv·h^{-1} over China (Wang et al., 2023a), indicating active nighttime NO_3 chemistry at this site. This substantial production rate suggests the presence of an efficient nighttime oxidation pathway and helps explain the observed RO_2* levels. We have added this quantitative analysis and a more detailed discussion of NO_3 chemistry to Section 3.3 of the revised manuscript.

"… at night (Figure 4a). The relatively high level of RO_2* at night indicates the presence of a nighttime peroxy radical source possibly due to NO_3 chemistry oxidation. We found that the average NO_3 production rate ($P(NO_3)$) at night during the campaign was approximately 1.4 ppbv·h^{-1}, higher than the reported warm-season mean of 1.07 ± 0.38 ppbv·h^{-1} over China (Wang et al., 2023a), indicating active nighttime NO_3 chemistry at this site."

Minor Comments

Line 76: wording correction.
Thank you for the suggestion. The wording has been revised to "NO and CO are introduced to drive chain reactions that amplify peroxy radicals into detectable NO_2 signals."

Line 264: extra space.
Corrected accordingly.

Line 275: define abbreviations and use LOD.
Corrected accordingly.

Line 313: 'deceased' should be 'decreased'. O_3 range appears reversed.
Corrected accordingly.

Reference

Atkinson, R., Baulch, D. L., Cox, R. A., Crowley, J. N., Hampson, R. F., Hynes, R. G., Jenkin, M. E., Rossi, M. J., and Troe, J.: Evaluated kinetic and photochemical data for atmospheric chemistry: volume I - gas phase reactions of Ox, HO_x, NO_x and SO_x species, Atmos. Chem. Phys., 4, 1461–1738, https://doi.org/10.5194/acp-4-1461-2004, 2004.

Chen, Y., Yang, C., Zhao, W., Fang, B., Xu, X., Gai, Y., Lin, X., Chen, W., and Zhang, W.: Ultra-sensitive measurement of peroxy radicals by chemical amplification broadband cavity-enhanced spectroscopy, Analyst, 141, 5870–5878, https://doi.org/10.1039/C6AN01038E, 2016.

Duncianu, M., Lahib, A., Tomas, A., Stevens, P. S., and Dusanter, S.: Characterization of a chemical amplifier for peroxy radical measurements in the atmosphere, Atmos. Environ., 222, 117106, https://doi.org/10.1016/j.atmosenv.2019.117106, 2020.

George, M., Andrés Hernández, M. D., Nenakhov, V., Liu, Y., and Burrows, J. P.: Airborne measurement of peroxy radicals using chemical amplification coupled with cavity ring-down spectroscopy: the PeRCEAS instrument, Atmos. Meas. Tech., 13, 2577–2600, https://doi.org/10.5194/amt-13-2577-2020, 2020.

Green, T. J., Reeves, C. E., Brough, N., Edwards, G. D., Monks, P. S., and Penkett, S. A.: Airborne measurements of peroxy radicals using the PERCA technique, J. Environ. Monit., 5, 75–83, https://doi.org/10.1039/b204493e, 2003.

Horstjann, M., Andrés Hernández, M. D., Nenakhov, V., Chrobry, A., and Burrows, J. P.: Peroxy radical detection for airborne atmospheric measurements using absorption spectroscopy of NO_2, Atmos. Meas. Tech., 7, 1245–1257, https://doi.org/10.5194/amt-7-1245-2014, 2014.

Kartal, D., Andrés-Hernández, M. D., Reichert, L., Schlager, H., and Burrows, J. P.: Technical note: characterisation of a DUALER instrument for the airborne measurement of peroxy radicals during AMMA 2006, Atmos. Chem. Phys., 10, 3047–3062, https://doi.org/10.5194/acp-10-3047-2010, 2010.

Liu, Y. and Zhang, J.: Atmospheric peroxy radical measurements using dual-channel chemical amplification cavity ringdown spectroscopy, Anal. Chem., 86, 5391–5398, https://doi.org/10.1021/ac5004689, 2014.

Liu, Y., Morales-Cueto, R., Hargrove, J., Medina, D., and Zhang, J.: Measurements of peroxy radicals using chemical amplification-cavity ringdown spectroscopy, Environ. Sci. Technol., 43, 7791–7796, https://doi.org/10.1021/es901146t, 2009.

Situ, S., Guenther, A., Wang, X., Jiang, X., Turnipseed, A., Wu, Z., Bai, J., and Wang, X.: Impacts of seasonal and regional variability in biogenic VOC emissions on surface ozone in the pearl river delta region, china, Atmos. Chem. Phys., 13, 11803–11817, https://doi.org/10.5194/acp-13-11803-2013, 2013.

Stone, D., Evans, M. J., Commane, R., Ingham, T., Floquet, C. F. A., McQuaid, J. B., Brookes, D. M., Monks, P. S., Purvis, R., Hamilton, J. F., Hopkins, J., Lee, J., Lewis, A. C., Stewart, D., Murphy, J. G., Mills, G., Oram, D., Reeves, C. E., and Heard, D. E.: HO_x observations over west Africa during AMMA: impact of isoprene and NO_x, Atmos. Chem. Phys., 10, 9415–9429, https://doi.org/10.5194/acp-10-9415-2010, 2010.

Sun, J., Yu, X., Ling, Z., Fang, G., Ming, L., Zhao, J., Zou, S., Guan, H., Wang, H., Wang, X., Wang, Z., Gao, Y., Tham, Y. J., Guo, H., and Zhang, Y.: Roles of photochemical consumption of VOCs on regional background O3 concentration and atmospheric reactivity over the pearl river estuary, southern China, Sci. Total Environ., 928, 172321, https://doi.org/10.1016/j.scitotenv.2024.172321, 2024.

Wang, H., Wang, H., Lu, X., Lu, K., Zhang, L., Tham, Y. J., Shi, Z., Aikin, K., Fan, S., Brown, S. S., and Zhang, Y.: Increased night-time oxidation over China despite widespread decrease across the globe, Nat. Geosci., 16, 217–223, https://doi.org/10.1038/s41561-022-01122-x, 2023a.

Wang, J., Zhang, Y., Xiao, S., Wu, Z., and Wang, X.: Ozone formation at a suburban site in the pearl river delta region, china: role of biogenic volatile organic compounds, Atmosphere, 14, 609–625, https://doi.org/10.3390/atmos14040609, 2023c.

Wolfe, G. M., Marvin, M. R., Roberts, S. J., Travis, K. R., and Liao, J.: The framework for 0-D atmospheric modeling (F0AM) v3.1, Geosci. Model Dev., 9, 3309–3319, https://doi.org/10.5194/gmd-9-3309-2016, 2016.

Wood, E. C. and Charest, J. R.: Chemical amplification - cavity attenuated phase shift spectroscopy measurements of atmospheric peroxy radicals, Anal. Chem., 86, 10266–10273, https://doi.org/10.1021/ac502451m, 2014.

Wood, E. C., Deming, B. L., and Kundu, S.: Ethane-based chemical amplification measurement technique for atmospheric peroxy radicals, Environ. Sci. Technol. Lett., 4, 15–19, https://doi.org/10.1021/acs.estlett.6b00438, 2017.